ELSEVIER

Reliability Engineering and System Safety 70 (2000) 15–27

RELIABILITY ENGINEERING & SYSTEM SAFETY

www.elsevier.com/locate/ress

Combination of finite element and reliability methods in nonlinear fracture mechanics

M. Pendola[a,*], A. Mohamed[b], M. Lemaire[b], P. Hornet[a]

[a]*EDF-DRD, Mechanics and Technology Department, 77818 Moret-sur-Loing Cedex, France*
[b]*LaRAMA-IFMA/UBP, BP 265, 63175 Aubiere Cedex, France*

Received 27 July 1998; accepted 15 March 2000

Abstract

This paper presents a probabilistic methodology for nonlinear fracture analysis in order to get decisive help for the reparation and functioning optimization of general cracked structures. It involves nonlinear finite element analysis. Two methods are studied for the coupling of finite element with reliability software: the direct method and the quadratic response surface method. To ensure the response surface efficiency, we introduce new quality measures in the convergence scheme. An example of a cracked pipe is presented to illustrate the proposed methodology. The results show that the methodology is able to give accurate probabilistic characterization of the *J*-integral in elastic–plastic fracture mechanics without obvious time consumption. By introducing an "analysis re-using" technique, we show how the response surface method becomes cost attractive in case of incremental finite element analysis.

Keywords: Structural reliability; Direct coupling method; Quadratic response surface method; Pipe; Finite element analysis; Nonlinear fracture mechanics

1. Introduction

The finite element method represents the most important tool for structural analysis and design. Its applications are increasing and its progress offers solutions to a wide variety of problems such as three-dimensional (3D) structural analysis and nonlinear behavior. In the meantime, methods based on the probability theory have also been put forward to try to quantify the influence of data uncertainties. They now offer some techniques of practical application by introducing some approximations in the mechanical systems where the validity domain can be well defined.

In case of cracked components, the Linear Elastic Fracture Mechanics theory (LEFM) and the Elastic–Plastic Fracture Mechanics (EPFM) provide accurate deterministic relationship between the maximum allowable external loading and the component parameters: dimensions, material properties, crack size and location. However, due to uncertainties in some of these parameters (for instance, crack size and material properties), a purely deterministic approach provides an incomplete picture of the reality. Therefore, a probabilistic approach seems to be very helpful for practical engineering and especially for the nuclear field: with the goal to decide when a repair is necessary, it is interesting to know the probability of failure of a damaged structure subjected to a possible accidental load effect. Such approaches, named *probabilistic fracture mechanics* are then particularly interesting for taking into account the uncertainties related to the structure during the stage of design or in operation to optimize the functioning conditions.

In many cases, the structural load effect cannot be expressed explicitly and some finite element calculations are necessary. Coupling of finite element analyses (FEA) with reliability methods is therefore necessary but implies difficulties such as prohibitive computation effort.

This paper deals with the case of coupling nonlinear fracture models with reliability methods, that is to say showing the interest of performing a complex mechanical study in a reliability context. From a mechanical point of view, only static behavior is considered and the reliability model concerns random variables but not random fields and time indexed stochastic processes.

The nonlinear fracture model is presented in the scope of the analysis of an axisymmetrically cracked pipe under pressure and tension with confined plastic behavior (i.e. the ligament is not fully plastified). Two reliability methods are used in the evaluation of the pipe safety: direct coupling and Quadratic Response Surface (QRS) method. This problem has been analyzed by other authors (see for

* Corresponding author. Tel.: +33-1-6073-7748; fax: +33-1-6073-6559.
E-mail address: maurice.pendola@edf.fr (M. Pendola).

0951-8320/00/$ - see front matter
PII: S0951-8320(00)00043-0

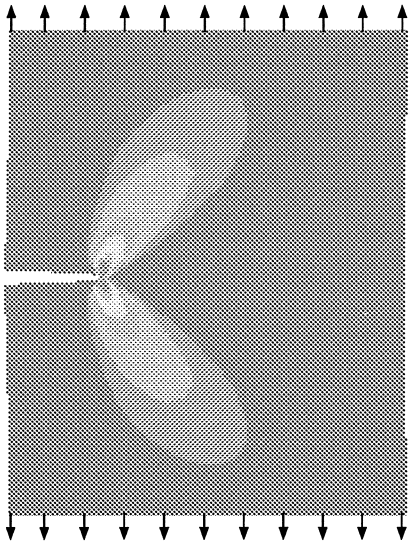

Fig. 1. Plastic zone in ductile fracture mechanics.

example Ref. [6]), but here emphasis is laid on the computation costs that can be largely decreased by optimal re-using of all the incremental analysis performed in the finite element code due to the nonlinear behavior. We also propose some measures for the precision of the approximated response. The results from this example show that the methodology is able to give accurate probabilistic characterization of the structure integrity in the field of elastic–plastic fracture mechanics. Contrary to single reliability analysis, the efficiency of the QRS method is proven in parametric analysis which is very interesting in real industrial projects.

2. Mechanical model

2.1. General assumptions

Many existing structures or mechanical components have cracks resulting from their manufacture (metallurgical factors) or from their use (mechanical factors) which may lead to the fracture of the structure. A crack is a geometrical discontinuity which modifies stress, strain and displacement fields so that the homogeneity of the material would not make sense. Here we are essentially interested in a particular type of nonlinear fracture: the ductile fracture which concerns materials where crack growth goes with plasticity. The fracture is said to be ductile if we can show a stable crack growth instead of fracture by instability. The word "stable" is used here to denote that the crack does not grow if the external loading is maintained constant. Moreover this fracture model goes with important plastic strains in the region where the crack appears and grows (see Fig. 1).

So, we should take into account the effects of plasticity in order to get more accurate and more realistic modeling of the crack growth. For the description of the material behavior in the elastic–plastic range, a general assumption is taken in the nuclear field and adopted here: it is to write the 1D stress–strain relationship as a power law (the Ramberg–Osgood law)

$$\epsilon = \frac{\sigma}{E} + \alpha \frac{\sigma_y}{E} \left(\frac{\sigma}{\sigma_y} \right)^n \tag{1}$$

where ϵ is the strain, σ the applied stress, E the Young's modulus, σ_y the reference stress which may be arbitrary, but is usually assumed to be the yield strength, n the strain hardening coefficient and α the coefficient of the Ramberg–Osgood law. These coefficients are parameters usually chosen from the best fit of laboratory data.

From a practical point of view, the stress–strain curve is defined through a piecewise form in the finite element software, as shown in Fig. 2.

The first segment is deduced from the linear relationship $\epsilon = \sigma/E$, the others are deduced from Eq. (1) using increments of 50 MPa. In case of multiaxial loading, the Von Mises criterion is used.

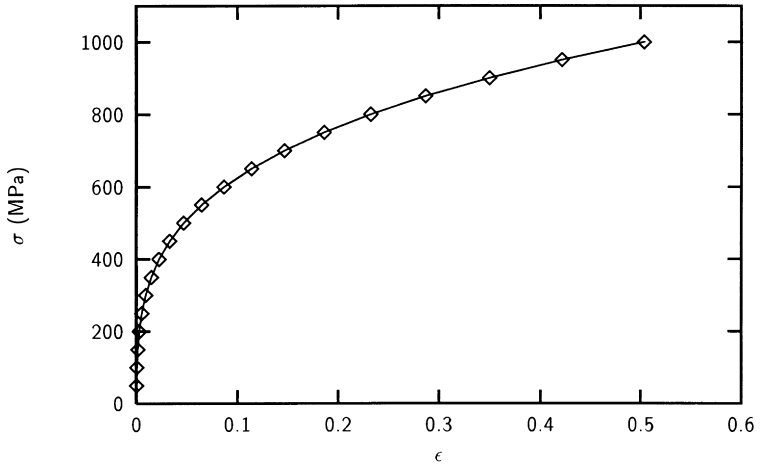

Fig. 2. Stress–strain curve adopted in the finite element software.

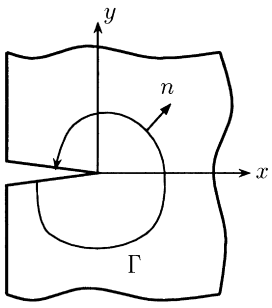

Fig. 3. Integration path surrounding the crack tip.

2.2. Loading effect characterization

There are several ways to characterize the stress field singularity in the vicinity of the crack tip [27]: exact solutions are only known for special cases but the developments based on the energy conservation laws are particularly interesting for nonlinear fracture mechanics. The crack growth is governed by the strain energy release rate indicating the energy dissipation during the material separation (i.e. breaking of cohesive forces between particles). In the general case, the *J*-integral, whose formulation is based on energy considerations, is a very good measure of the crack driving forces [12,25]. In nonlinear behavior, the *J*-integral is known to be path independent as long as the path remains far enough from the plastic region and loading is monotonic increasing (local unloading is not taken into account). Eq. (2) gives the expression of the *J*-integral in 2D form [25]. It assumes that the crack lies in the global Cartesian x–y plane, with the x-axis parallel to the crack (see Fig. 3)

$$J = \int_{\Gamma} W \, \mathrm{d}y - \int_{\Gamma} \left(t_x \frac{\partial u_x}{\partial x} + t_y \frac{\partial u_y}{\partial y} \right) \mathrm{d}s \qquad (2)$$

where Γ is any path surrounding the crack tip, W is the strain energy density (i.e. strain energy per unit volume), t_x the tension vector along x-axis ($= \sigma_x n_x + \sigma_{xy} n_y$), t_y the tension vector along y-axis ($= \sigma_y n_y + \sigma_{xy} n_x$), σ the stress components, n the unit outer normal vector to the path Γ, u the displacement vector, and s the distance along the path Γ.

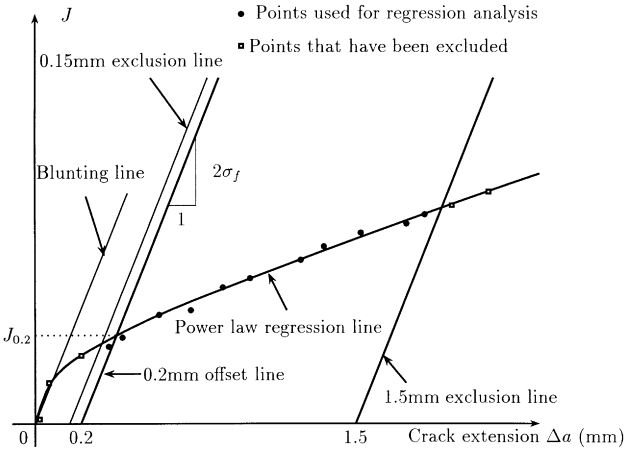

Fig. 4. Definition of $J_{0.2}$ according to ASTM E 813 [3].

2.2.1. Finite element implementation

2.2.1.1. Meshes associated with fracture modeling. One of the greatest difficulties in fracture mechanics is the mesh refinement which has to account for the singular stress and displacement fields at the crack tip. The evaluation of the *J*-integral needs a high precision which implies adapted meshing:

- either a refined mesh which converges at the crack tip. We can use quadratic elements at the crack tip with length between 1/500 and 1/50 of the crack length;
- or the use of Barsoum's elements where the midside nodes are placed at the quarter points. Such elements induce the same singularity as the searched fields.

2.2.1.2. Numerical evaluation of the J-integral. The *J*-integral computation is carried out by the software ANSYS [2] and *Code_Aster* [7] in order to have a validation of the mechanical results by comparison.

With ANSYS, the *J*-integral is directly evaluated by considering Eq. (2):

- The path is chosen far enough from the crack tip to avoid errors due to the singularity.
- The derivatives of the displacement vector are calculated by shifting the path a small distance in the positive and negative X directions.
- The stresses and the strains are evaluated along the path Γ defined by nodes, that is to say we use an interpolation process from the known values at the Gauss points.

With the software *Code_Aster* [7], the crack driving force evaluation is implemented through the use of the θ-method developed by the French company Electricite de France (EDF). This method considers the exact derivatives of the displacement field by rewriting the variational formulations.

2.3. Characterization of the structural strength

In order to evaluate the structural integrity, relevant failure criteria must be defined. Two definitions are commonly used in the EPFM [14]: (i) initiation of crack growth; and (ii) unstable crack growth. The initiation of crack growth in a structure containing flaws is observed when the crack driving force J exceeds the material toughness (J_{Ic}) depending only on the material. This criterion is commonly used in piping and pressure vessel analyses [23]. Otherwise this criterion provides a conservative estimate of the structural integrity because after crack growth initiation there is unstable crack growth. This criterion is used in the current fracture analysis.

The crack initiation in ductile elastic-plastic environments

is thus obtained when Rice's integral reaches the material toughness $J_{0.2}$. This value results from experimentation. The index 0.2 means 0.2 mm, i.e. the toughness is defined for a 0.2 mm crack propagation. $J_{0.2}$ is then the value defined by the intersection between the regression curve due to the experimental points and the parallel to the blunting line defined by the equation $J = 2\sigma_f \Delta a$ (Fig. 4) where σ_f is the flow stress defined by the mean of the yield stress and the maximal stress.

2.4. Remarks on mechanical modeling

Fracture mechanics is based on assumptions and formulations which may lead to accurate and realistic modeling of the cracking phenomena but which still requires heavy computation efforts. The main problem is therefore to pilot the finite element calculations in a nonlinear context when a parametric reliability analysis has to be performed (multiplication of the FEA computations is required). As single FEA requires several minutes and as the expected probability of failure is generally very small, the classical Monte Carlo simulations cannot be reasonably used. Special coupling approaches for reliability methods and finite element analyses have to be considered.

3. Coupling finite element with reliability methods

The main reliability methods used in our study are based on FORM/SORM (First/Second Order Reliability Methods). Different approaches have been proposed and two of them are used here. The first one is based on the computation of the Hasofer and Lind β index [17] for an approximate form of the loading effect given by a response surface. The second approach is based on a direct computation of the reliability index using FEA by optimization procedures. This second method which requires a link between the finite element and reliability software has been essentially used to validate the first one which does not need significant programming cost.

3.1. Reliability problem—notations

Let x_i be a realization of the random variable X_i (i varying from 1 to the number of basic variables N) and $G(x_i)$ the performance function

$G(x_i) > 0$ is a success realization, $x_i \in D_s$, safety domain;
$G(x_i) \leq 0$ is a failure realization, $x_i \in D_f$, failure domain;
$G(x_i) = 0$ is the limit state.

The probabilistic transformation T gives for any physical vector X_i, the standardized vector U_j of Gaussian variables $\mathcal{N}(0,1)$. The Nataf transformation [8], that requires only limited information (generally available) on variables X_i (marginal densities and correlation), constitutes an efficient solution. It is thus

$$u_i = T_i(x_j) \qquad G(x_i) = G(T_i^{-1}(u_j)) \equiv H(u_j) \tag{3}$$

The Hasofer–Lind reliability index β is then calculated by solving the optimization problem

$$\beta = \min \left(\sqrt{\sum_{i=1}^{N} u_i^2} \right) \qquad \text{under the constraint } H(u_i) \leq 0 \tag{4}$$

The solution gives the value of β and the coordinates u_i^* of the design point P^* as well as the direction cosines α_i (sensitivity factors in the standardized space).

3.2. Direct coupling method

By the *direct coupling method*, we mean any reliability procedure based on a β-point search algorithm using directly the FEA each time the limit state function has to be evaluated. The β-point search can be carried out by any optimization method allowing to solve Eq. (4).

By using the gradient based algorithms, there is no need to know the closed-form of the limit state function to determine the failure probability. All that we need are the values of the limit state and its gradient (and may be the Hessian) at the computation points. Historically, the Rackwitz and Fiessler algorithm [22] has been frequently used in reliability analysis but some instability problems were observed. The convergence rate has been well improved by the Abdo and Rackwitz algorithm which is a simplified form of the sequential quadratic programming algorithm [1]. As for the most of optimization methods, there is no guarantee that the calculated minimum is really the global minimum of the problem; only good engineering sense allows us to get a logical interpretation of the coherence of the failure configuration.

3.3. Quadratic response surface method

In many industrial cases, the structural failure cannot be defined by an explicit function of the random variables; only an implicit definition of the limit state G is available. The solution can be obtained by the construction of the response surface (RS) based on a limited number of realizations in order to obtain the approximation of the limit state function. The use of response surfaces in reliability problems is not recent, but has not been achieved and new contributions are always proposed. Works have defined concepts [5,11,19,24], built solutions in the physical space [4], proposed methods of evolution [10,13] and showed applications with finite element coupling [6,26]. It is emphasized here on a method proposed by [9] and based on an approximation of the limit state in the vicinity of the design point determined after successive iterations.

3.3.1. Quadratic response surface evaluation

The main idea of the response surface method is to build a

polynomial expansion of the limit state function $G(x_i)$ or $H(u_i)$. The degree 2 (Quadratic Response Surface, QRS) is the best solution since it includes a possible calculation of curvatures and it avoids possible oscillations of higher order polynomials. We choose to built the approximation in the standardized space. If there are N random variables in the standardized space, the approximation $\tilde{H}(u_i)$ of $H(u_i)$ can be written as

$$\tilde{H}(u_i) = c + \sum_{i=1}^{N} b_i u_i + \sum_{i=1}^{N}\sum_{j=i}^{N} a_{ij} u_i u_j \tag{5}$$

where c, b_i and a_{ij} are constants to be determined. The function $\tilde{H}(u_i)$ is defined by at least $r_{\min} = (N+1)(N+2)/2$ points but in practice a larger number r of points is taken and the approximation is obtained by minimizing the least squares

$$\sum_{l=1}^{r} |\tilde{H}(u_i^{(l)}) - H(u_i^{(l)})|^2 \tag{6}$$

At the iteration "h", the construction of the polynomial approximation is done by choosing carefully the set (k) of realizations of the implicit function $H(u_i)$. The equation $\tilde{H}(u_i) = 0$ enables us to calculate an estimation of $\beta^{(k)}$ and the most probable failure point ${u_i}^*$. A new polynomial approximation ($k+1$) is obtained from the evaluation of the implicit function located in the vicinity of $u_i^{*(k)}$ and eventually some of the previous realizations of the implicit function stored in the database. Several iterations allow us to approach the limit state function and to calculate the index β. The convergence is achieved, with the same conditions as in the direct coupling method, when

$$|\beta^{(k+1)} - \beta^{(k)}| \leq \epsilon_\beta \tag{7}$$

$$\left| \frac{H(\{u\}^{(k+1)})}{H(\{0\})} \right| \leq \epsilon_H \tag{8}$$

where ϵ_β and ϵ_H are, respectively, the convergence tolerance for β and H. To avoid error redistribution between the design point components, an additional condition should be applied on the normalized variable components

$$|u_i^{(k+1)} - u_i^{(k)}| \leq \epsilon_u \tag{9}$$

where ϵ_u is the convergence tolerance for u_i. The re-use of the nearest points obtained in the previous iteration decreases the number of finite element computations and thereby the global computation cost [21].

3.3.2. Quality of the RS

The main problem in the response surface analysis is the validation of the obtained results and approximations. There are tests giving measures on the quality of the approximations. They can be classified according to the necessary information for their evaluation [15]

- *Physically admissible realizations.* We build the response surface in the standard space. The choice of a realization $u_j^{(l)}$ implies a physical realization $x_i^{(l)} = T_i^{-1}(u_j^{(l)})$ that must be physically feasible and corresponds to a compatible situation with the mechanical model hypotheses. If not, the aberrant realization is excluded from the set of experiments. When the coefficients of variation are relatively small there is always a physical realization in the considered probability domain. This verification has to be performed only when the scatter of the variable is great in order to avoid aberrant computations.
- *Quality of the regression.* It is measured after the calculation of the realizations $\tilde{H}(u_i^{(l)})$. The measure is the correlation R^2 between real limit state and the polynomial approximation calculated at the points $u_i^{(l)}$

$$R^2 = 1 - \frac{\sum_{l=1}^{r} (H(u_i^{(l)}) - \tilde{H}(u_i^{(l)}))^2}{\sum_{l=1}^{r} (E[H(u_i^{(l)})] - H(u_i^{(l)}))^2} \to 1$$

  in which $E[\cdot]$ is the average. This measure is equal to 1 for an interpolation and must be used only to control the regression where a value superior to 0.95 is expected. If the statistic R^2 is less than 0.95, it means that the regression does not consider all the available information contained in the numerical experiments. In such cases, experience shows that taking into account more numerical experiments leads to better approximations.
- *Value of the limit state function.* At the end of the reliability calculation, the design point P^* is obtained. We propose two supplementary measures [21]
  - the first measure checks the belonging of P^* to the design of experiments

$$I_{\text{app}} = 1 - \left(\frac{1}{r} \sum_{t=1}^{j} \frac{N_t}{t!} \right)^{-1} \to 1$$

    where j is the chosen limit for the development and N_t is the number of the set of experiments points to be less than t standard deviations of P^* according to a given norm

$$N_t = \text{card}(P^{(l)} | \max_{i=1,N} (u_i^{(l)} - \tilde{u}_i^*) < t)$$

    or

$$N_t = \text{card}\left(P^{(l)} \middle| \sqrt{\sum_{i=1}^{N} (u_i^{(l)} - \tilde{u}_i^*)^2} < t\right)$$

  - the second measure verifies that the design point

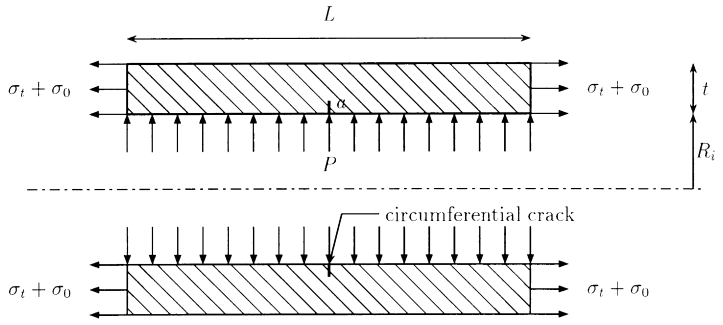

Fig. 5. Axisymmetrically cracked pipe.

belongs to the real limit state function (see Eq. (8))

$$I_a = \frac{H(\{\vec{u}^*\})}{H(\{0\})} \to 0$$

It requires a supplementary mechanical calculation and if it tests the belonging to the limit state, it does not prove that it is a minimum on the limit state function. However experience [21] shows that good reliability results are strongly correlated with a good measure of I_a, and reciprocally.

4. Application to a cracked pipe

4.1. Description of the pipe

The pipes of nuclear plants undergo great thermal and mechanical cycles which can lead to initiation and propagation of cracks. When a crack is observed, the problem is to know whether it is suitable to repair the structure as a priority or if it can be justified that an accident will not occur. Therefore, the reliability analysis can provide the failure probability knowing that there is a crack and that the load can reach accidental values defined in a particular range.

Fig. 5 shows an axisymmetrically cracked pipe under internal pressure and axial tension. Due to the boundary conditions at the pipe ends, the applied hydraulic pressure induces, beside the radial pressure, longitudinal tension forces.

The system variables are described as follows:

- a, the crack length (15 mm)
- L, the pipe length (1000 mm)
- P, the internal pressure (15.5 MPa)
- R_i, the inner radius (393.5 mm)
- t, the thickness (62.5 mm)
- σ_t, the applied tensile stress (varying from 100 up to 200 MPa). It represents the load effect which could accidentally increase, knowing that the nominal value is around 100 MPa. This load is taken as a deterministic parameter in the reliability analysis, that is to say we are interested in obtaining the failure probability as a function of the tensile stress in order to be able to decide if pipe repairing has to be done with acceptable failure probability for a given crack length and loading effect.
- σ_0, the stress due to the end effects, given by

$$\sigma_0 = P\frac{R_i^2}{(R_i + t)^2 - R_i^2}$$

4.2. Finite element model

4.2.1. Boundary conditions

Due to the symmetry of the problem (axisymmetry, crack loaded in the opening mode), we just consider the half of the pipe and we use quadratic isoparametric elements. The boundary conditions are shown in Fig. 6. The nodes located on the rim of the crack are free, the others are clamped in the direction of the tensile stress.

To carry out a parametric study in function of the tensile stress σ_t, we store in a database the results at each step of the incremental analyses corresponding to 5 MPa steps of σ_t.

The length of the pipe is chosen so that it does not induce interferences in the computation of Rice's integral.

4.2.2. Pipe mesh

It has been seen that the mesh geometry has to account for

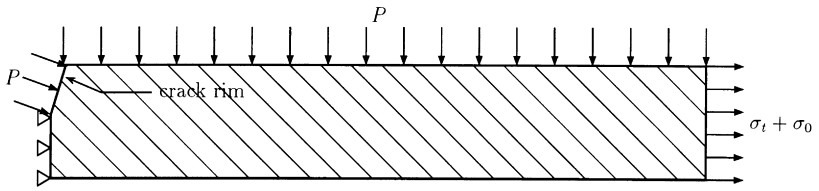

Fig. 6. Applied boundary conditions.

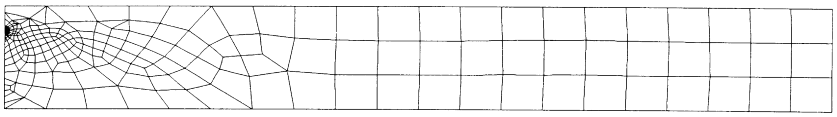

Fig. 7. Mesh used in the ANSYS software.

singular stress and displacement fields at the crack tip. The meshes used in the finite element software are presented in Figs. 5 and 6; they are compared in order to validate the models.

- *The ANSYS mesh.* We use quadratic elements (6- and 8-node elements) with the midside nodes placed at the quarter points in the vicinity of the crack. Fig. 7 shows the mesh used in the software ANSYS (363 elements and 1002 nodes).
- *The Code_ASTER mesh.* In *Code_ASTER*, only classical elements are used (axisymmetric isoparametric elements with 6 and 8 nodes) and the mesh is extremely refined in the vicinity of the crack tip with element length of 0.2 mm (1182 elements and 3327 nodes). This mesh can be seen in Fig. 8.
- *Comparison of the FE meshes.* As there are no Barsoum elements implemented in *Code_ASTER*, it has been chosen to perform a more refined mesh than with ANSYS. It has however to be noted that the mesh in *Code_ASTER* could have been optimized.

There is no theoretical solution of our problem in the nonlinear case, then the mesh's accuracy is measured on the basis of a linear analysis of a cracked plate under tension assuming plane stress conditions. The same mesh geometry with plane stress elements is therefore used. The fracture mechanics formulation in such a case gives theoretical results which can be compared with the finite element solutions. The obtained results and the corresponding discrepancies with the theory are summarized in Table 1. According to these results (the error does not exceed 0.3%), we can state that the accuracy of the meshes are satisfactory. Moreover, in terms of element types and *J*-integral evaluation in the two software, it is shown that the mechanical models are robust. A similar comparison in the elastic–plastic case for the nominal values of the input parameters shows that the discrepancy between the two numerical models does not exceed 1% which attests of their robustness in our case.

The mechanical model being validated and robust, the problem is then to couple it with reliability algorithms knowing that it can be very time consuming to perform a parametric study since a single finite element analysis needs more than 10 min.

4.3. Reliability estimation of the cracked pipe

We are interested in the evaluation of the failure probability of the cracked pipe shown in Fig. 5 as a function of the applied tensile stress σ_t. Depending on the location of the pipes in the nuclear plant, different materials are used. We are interested here in two aspects: first the reliability evaluation of a typical pipe made of a typical steel and the global reliability evaluation for all the pipes in the plant, i.e. with different material properties but assuming the same geometry.

4.3.1. Limit state formulation

In order to evaluate the structural integrity, the risk to be evaluated is given by the probability that the loading effect, defined by the crack driving force J, exceeds the structural strength given by $J_{0.2}$

$$P_f = \text{prob}(J \geq J_{0.2}) \tag{10}$$

The limit state function is written as

$$G(X_i) = J_{0.2} - J(E, \sigma_y, n, \alpha) \tag{11}$$

which is an implicit nonlinear function because J is evaluated by FEA.

4.3.2. Random variables, distributions and parameters

In this problem, five random variables are considered: the material toughness $J_{0.2}$ and the variables in the Ramberg–Osgood law (Young's modulus E, the yield strength σ_y, the strain hardening exponent n and the Ramberg–Osgood coefficient α). These random variables are assumed to be statistically independent.

In the first reliability analysis (i.e. the reliability of a typical pipe with given material properties), the random variables are described with parameters and distributions resulting from expert judgements; they are summarized in Table 2. In the second reliability analysis (i.e. global study of plant pipes), the distributions of the material properties are determined according to the material databases in order to reflect the material variability for all the plant pipes. As a

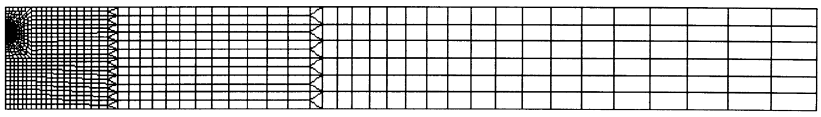

Fig. 8. Mesh used in *Code_ASTER*.

Table 1
Comparison with theoretical results

	Theory	ANSYS	Discrepancy (%)	Code_ASTER	Discrepancy (%)
Stress intensity factor K_I (MPa mm$^{-1/2}$)	1006.4	1003.6	−0.3	1007.0	0.1
Rice's integral J (MPa mm)	5.7715	5.7514	−0.3	5.7786	0.1

result, the means and the standard deviations of the random variables are different as shown in Table 3. For a given value of all the deterministic parameters, the limit state function can now be written as a function of the random variables:

$$G(J_{0.2}, E, \sigma_y, n, \alpha) = J_{0.2} - J(E, \sigma_y, n, \alpha) \tag{12}$$

4.3.3. Implementation of the coupling schemes

4.3.3.1. Coupled software

- *ANSYS* [2] is a general finite element software which solves the most of mechanical and thermal problems. Its qualities are well known and it is widely used in the industry.
- *RYFES* [18] is a *reliability base design* software developed by the LaRAMA. It allows us to perform the reliability analysis with virtually any standard finite element software, by using the direct methods, the response surface methods and the Monte Carlo simulations.
- *Code_ASTER* [7] is a general finite element code developed by the company EDF to fit exactly the needs of finite element simulations of its products.
- *PROBAN* [20] is a general reliability software developed by Det Norske Veritas. It is able to perform the general cases of reliability estimation encountered in the industry.

We are therefore using two different coupling strategies with two different finite element codes and two different reliability software; this can be seen in Fig. 9.

4.3.3.2. Direct coupling with RYFES and ANSYS (case A). In the direct coupling scheme, the reliability software should be able to pilot the FEA software. This implies that the design variables are transparent in both models. The main computation effort is due to the FEA while the convergence rate is due to the reliability analysis.

As it has been mentioned, RYFES is a general purpose software, which is developed to be used in the practical engineering field. The direct coupling with the FEA software ANSYS has the advantage of extending the reliability analysis to a wide range of mechanical problems: static, dynamic, transient, nonlinear, thermal, magnetic, etc. In the coupling context, the software ANSYS has the advantage of having a complete "parametric language" and an optimization procedure. Fig. 10 shows the RYFES–ANSYS coupling scheme. The classical deterministic file is imported into RYFES which recognizes automatically all the model variables and their interactions, then creates special reliability database files. By the mean of graphical windows, the probabilistic model and the limit state can easily be defined. RYFES creates new instruction files and pilots the FE analyses by any one of the specified algorithms. The dialogue between mechanical and reliability procedures is performed through the ANSYS optimization procedure. At the convergence point, the ANSYS results are analyzed by RYFES in order to calculate the failure probability, the design point and the sensitivity measures.

4.3.3.3. Response surface coupling with PROBAN and Code_Aster (case B). The response surface method is applied herein to evaluate Rice's integral. The approximation is made by a full quadratic form of the random variables in the standard space

$$\tilde{J}(E, \sigma_y, n, \alpha) = c + \sum_{i=1}^{4} b_i u_i + \sum_{i=1}^{4} \sum_{j=i}^{4} a_{ij} u_i u_j \tag{13}$$

where c, b_i and a_{ij} are the constants to be evaluated and u_i is a normally distributed variable given by Nataf's probabilistic transformation T [17] of the variable x_i. In our case the function is defined at least by $(N+1)\times(N+2)/2 = 15$ points where N is the number of random variables in Rice's integral. In practice, we take a larger

Table 2
Random variables for the studied steel

Variable	Density law	Mean	Standard deviation
$J_{0.2}$ (MPa mm)	Lognormal	52	9.5
E (MPa)	Lognormal	175,500	10,000
σ_y (MPa)	Lognormal	259.5	10
n	Normal	3.5	0.1
α	Normal	1.15	0.15

Table 3
Random variables for all the plant steels

Variable	Density law	Mean	Standard deviation
$J_{0.2}$ (MPa mm)	Lognormal	76	7.6
E (MPa)	Lognormal	175,500	10,000
σ_y (MPa)	Lognormal	200	10
n	Normal	5.0	0.5
α	Normal	1.5	0.2

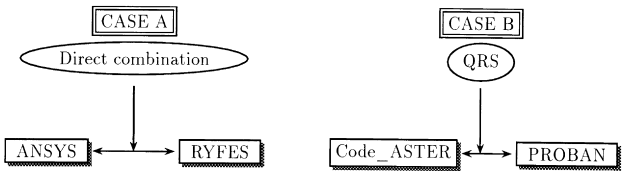

Fig. 9. Coupling implementations for the pipe reliability analysis.

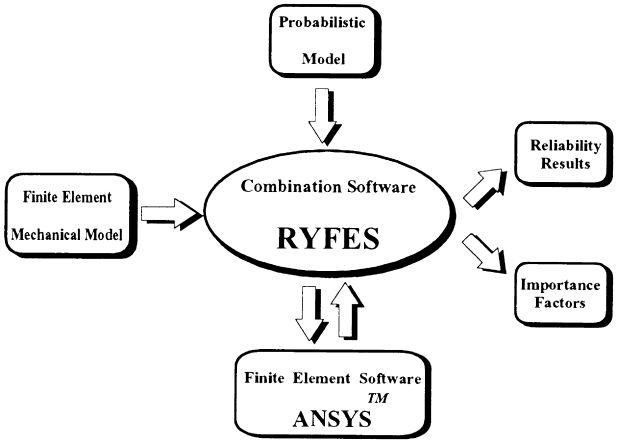

Fig. 10. RYFES–ANSYS coupling scheme.

number r of points and the approximation is obtained by regression.

4.4. Reliability results

4.4.1. Comparison of direct coupling and QRS results

Fig. 11 shows the evolution of the failure probability of the pipe versus the applied tensile stress obtained by the two mentioned coupling methods when using the typical steel properties. It is shown that both methods give the same failure probability level (in a wide range of probability: 10^{-10} up to 1) which allows us to rely on the obtained results. This conclusion concerns the results relative to the global steel database too (Fig. 12) although the maximal discrepancy reaches approximately one decade when the probability is very small (less than 10^{-9}).

Referring to this and knowing the crack length, we can decide whether the repairing of the pipe has to be made in an emergency or if it can wait. Conversely, if an acceptable failure probability level is decided, the curve shows the allowable load that the structure should support. For example, an acceptable risk of failure of 10^{-2} corresponds to a tensile stress of nearly 150 MPa for the typical steel and a tensile stress of 130 MPa for all the other pipes. As a conclusion, the pipes made with the typical steel have no restrictive effects, i.e. we can load them until 150 MPa without going over a probability of failure of 10^{-2} but they become less safe than for the nominal loading, i.e. around 100 MPa.

In our case, adding the crack length in the parameters of the failure probability evolution could for instance, point out an allowable crack length under a certain load. Such results are important for the operator to optimize the functioning conditions of the installation with a certain level of reliability.

Figs. 13 and 14 show that we obtain the same results for the coordinates of the design point with different coupling methods and with different finite element software. The maximum discrepancy concerns the values in distribution tails and for the most important variables (probabilistically speaking).

For each value of the applied tensile stress, the evaluated failure probability and the design point coordinates show that the results are the same. It is therefore proved by comparison that the results are validated.

4.4.2. Methodology for the QRS coupling scheme

For a given value of the applied stress, the main reliability results are the failure probability, the design point and the importance factors (by importance factors we mean the squared values of the directional cosines in the standardized space). The parametric analyses are performed at each

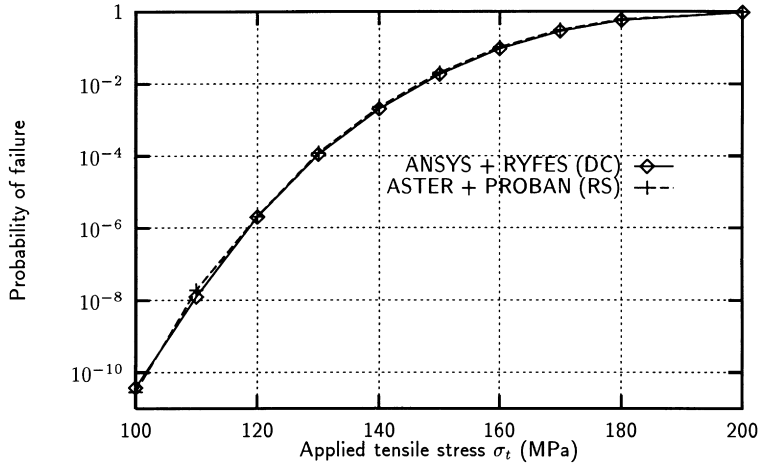

Fig. 11. Reliability results for the typical steel.

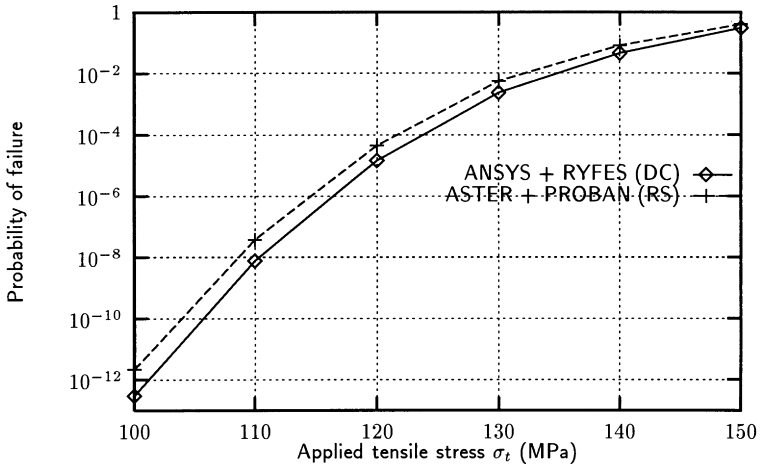

Fig. 12. Reliability results for the global steel database.

chosen level of the applied stress. They are therefore performed from 100 up to 200 MPa in an increasing order.

Let us illustrate the proposed methodology for the tensile stress value: $\sigma_t = 120$ MPa. In the case of direct coupling, the results relative to the typical steel are given in Table 4. These results are taken as a reference for the QRS coupling method.

According to Eq. (12), the resistance and the loading parts are dissociated, and a response surface is constructed for the second term only. At $\sigma_t = 120$ MPa, we use 20 experiments from the database resulting from the previous computations ($\sigma_t = 100$ and 110 MPa); the reliability computation on the resulting response surface is given in Table 5. The measure R^2 is satisfactory but I_{app} and I_a are not: the chosen experiments are far from the design point (referring to I_{app}) which means that this design point does not belong to the real limit state (see I_a). A second regression is then performed by undertaking five new experiments in the neighborhood of the found design point. These five experiments are joined to the 15 nearest experiments from the database, in order to construct the new response surface; Table 6 shows the obtained results. In this iteration, all the convergence criteria are fulfilled, all the measures are satisfactory and the results are the same compared to those obtained from the case A. The discrepancies concern the design point coordinates and they do not exceed 0.1 in the standardized space, that is to say nearly 10% of the standard deviation of the concerned variable. As the coefficient of variation of the concerned variable is 30%, the maximal discrepancy is about 3% (see Fig. 13).

These results needed only five new FEA, instead of 20. This is permitted by optimally re-using the database of experiments constructed in the previous computations (for $\sigma_t = 100$ and 110 MPa).

4.5. Validation of the QRS methodology

For all the values of the applied tensile stress, the results show that the toughness $J_{0.2}$ is the most important variable, probabilistic speaking. This is mainly due to its great

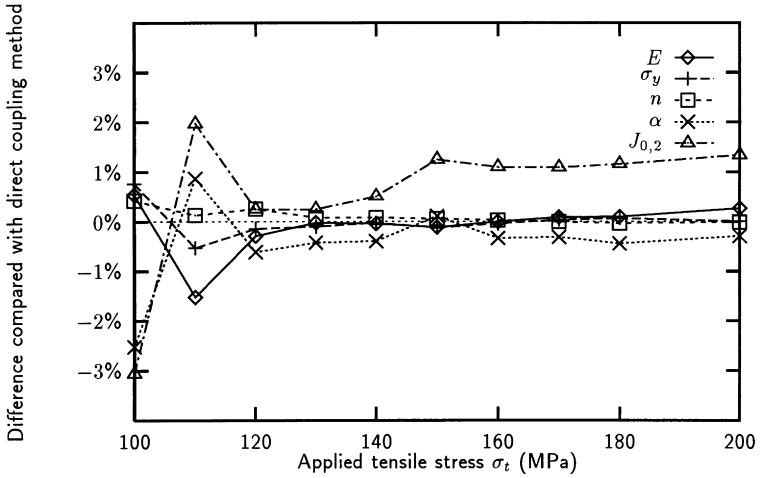

Fig. 13. Variation of the design point coordinates (typical steel).

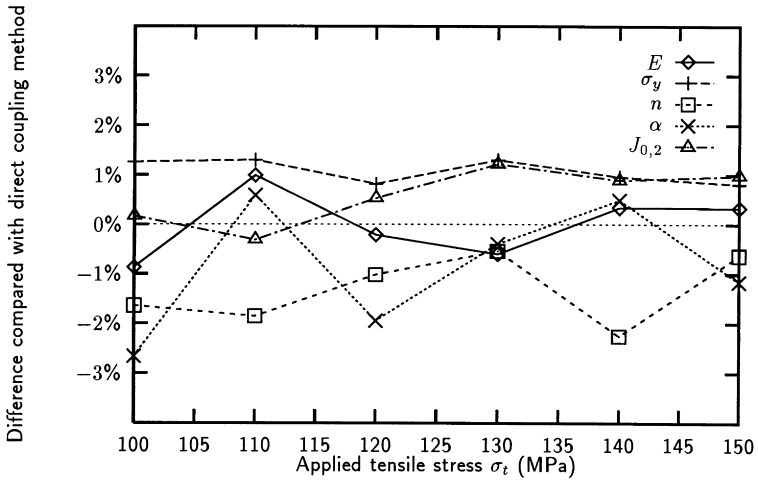

Fig. 14. Variation of the design point coordinates (steel database).

coefficient of variation. For example, according to this, the designer can concentrate the quality controls on this variable which contributes the most in the failure of the structure. The high importance of the toughness implies that one might put, without serious error, the variables in the *J*-integral (i.e. E, σ_y, n, α) to their mean values: an evaluation of the omission factor [16] would have probably shown that this factor is close to 1. In any case, despite the minor importance of the loading effect for the typical steel, the design point coordinates obtained with the response surface show that this method is able to fit accurately the real limit state in the vicinity of the design point, that is to say in the region of main interest (see Ref. [26]).

The accuracy of the QRS methodology is confirmed by the reliability analysis of the global steel database where the loading importance is nearly 80% (Fig. 15). The response surface is proven to be suitable for accurate representation of the contribution of the *J*-integral variables (i.e. E, σ_y, n, α). In this case, the yield stress σ_y becomes the most important variable (nearly 60%). Its nonlinear effect given in the Ramberg–Osgood law does not perturb the response surface method. The adaptive FEA re-using technique showed a very high performance.

4.6. Efficiency of the QRS method

The response surface method needs more than 15 finite element analyses to obtain the failure probability for a given applied stress (let us take 25 FEA to get accurate results). In compensation, to perform the complete parametric study as shown in Fig. 11 (computation for 10 values of the applied tensile stress), about 60 finite element analyses have been performed. As it has be shown in the above sections, to

Table 4
Reliability results for $\sigma_t = 120$ MPa by direct coupling

Variable	U^*	X^*	Importance factors (%)
$P_f = 2.01 \times 10^{-6}$			
$\beta = 4.61$			
$J_{0.2}$	−4.197	23.91	82.5
E	−1.276	162,930	8.3
σ_y	−0.886	250.61	4.0
n	−0.151	3.48	0.0
α	1.098	1.31	5.2

Table 5
Reliability results at the first iteration of case B ($\sigma_t = 120$ MPa)

Variable	U^*	X^*	Importance factors (%)
$P_f = 1.11 \times 10^{-6}$			
$\beta = 4.73$			
$J_{0.2}$	−4.30	23.48	82.6
E	−1.36	162,160	8.3
σ_y	−0.93	250.23	4.0
n	−0.08	3.49	0.0
α	1.10	1.32	5.1
Measures			
$R^2 = 98.5\%$			
$I_{app} = -23.46$			
$I_a = 3\%$			

Table 6
Reliability results at the second iteration of case B ($\sigma_t = 120$ MPa)

Variable	U^*	X^*	Importance factors (%)
$P_f = 2.07 \times 10^{-6}$			
$\beta = 4.61$			
$J_{0.2}$	−4.183	23.97	82.5
E	−1.325	162,480	8.3
σ_y	−0.923	250.25	4.0
n	−0.061	3.49	0.0
α	1.047	1.31	5.2
Measures			
$R^2 \approx 100\%$			
$I_{app} = -5.32$			
$I_a = 0.003\%$			

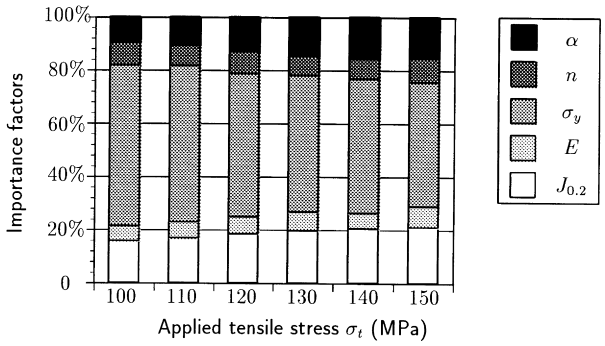

Fig. 15. Evolution of the importance factors for the whole steel database.

construct the response surface at a given loading level, we re-use the finite element computations performed at the previous stress levels.

For a given applied stress, the direct coupling method needs about five iterations which represents 30 finite element computations (because the response gradient is evaluated by finite difference technique), that is to say about 300 calculus for the whole curve of Fig. 11.

This great computation number can be greatly decreased by programming the gradient operators in the finite element software and by making the convergence criteria more flexible (leading to less precision). Even if we imagine that the number of the direct coupling iteration could be reduced to 2 (which is the minimum), the calculation of the probability curve in Fig. 11 requires at least 120 finite element computations, i.e. number of iterations $\times$ (1 + number of random variables) $\times$ number of tensile stress values.

To conclude, the response surface methodology reported here can be interesting in nonlinear finite element computations because it allows us to re-use optimally the incremental analysis. Refer to Fig. 16 for the main computation costs in our case, i.e. the cumulated number of finite element calls assuming that the first reliability estimation is made for $\sigma_t = 100$ MPa and that the number of the direct coupling method iterations can be reduced by a factor of 10 (nearly 60 FEA for QRS instead of 600 FEA for the *direct coupling*). The same reduction of the finite elements analyses can be expected in applications where the failure probability at each date in a transient analysis has to be evaluated. This is due to the storage in a database of all the performed calculations.

5. Conclusions

The first goal aimed at in this paper is to demonstrate the ability of performing a reliability analysis combined with a complex nonlinear mechanical model without using specific FEA software.

Fracture mechanics, with ductile material behavior is a relevant situation including plasticity and nonlinearity. Two theoretical models and two numerical implementations lead to sufficiently close results and attest the quality of the solution of the mechanical model.

In the same goal of comparison, two coupled mechanical and reliability approaches are shown. The direct method requires a strong link between mechanical and reliability procedures while the response surface method necessitates only a weak link through a database. Moreover, in the case of parametric study, it becomes more attractive: the computation costs can be consequently decreased by optimally reusing the incremental results stored in the database. The reusing strategy is based on the definition of quality measures of the response surface. The proposed methodology represents a balanced efficiency/precision scheme.

The second goal is to aid the designer to reach a decision in an industrial context. Indeed, he/she can decide whether to repair the structure before too high a level of risk appears or can wait for repair knowing that there is a limited risk of failure.

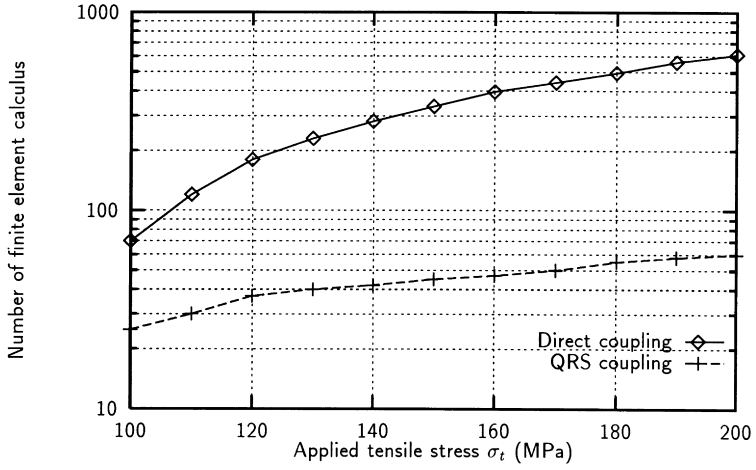

Fig. 16. Finite element calls in the two coupling methods.

References

[1] Abdo T, Rackwitz R. A new beta-point algorithm for large time-invariant and time variant reliability problems. Third WG IFIP Working Conference, Berkeley, 1990.

[2] Ansys, Inc. ANSYS 5.5—Finite Element Software, User's Manual, 1999.

[3] ASTM. Standard test method for J_{Ic}, a measure of fracture toughness. Annual Book of ASTM Standards, 0301, 1989.

[4] Bucher CG, Bourgund U. A fast and efficient response surface approach for structural reliability problems. Struct Safety 1990;7:57–66.

[5] Casciati F, Colombi P. In: Spanos PD, Wu YT, editors. Fatigue lifetime prediction for uncertain systems, Berlin: Springer, 1994.

[6] Colombi P, Faravelli L. In: Guedes Soares C, editor. Stochastic finite elements via response surface: fatigue crack growth problems, Dordrecht: Kluwer Academic, 1997.

[7] DER-EDF. Manuel d'Utilisation et Manuel de Référence de Code_ASTER. Electricité de France, 1995.

[8] Der Kiureghian A, Liu PL. Structural reliability under incomplete probability information. J Engng Mech 1986;112(1):85–104.

[9] Devictor N, Marques M, Lemaire M. Adaptative use of response surfaces in the reliability computations of mechanical components. In: Guedes Soares C, editor. Advances in safety and reliability, vol. 2. Amsterdam: Elsevier, 1997. p. 1269–77 (ESREL'97, Lisbon 17–20 June).

[10] Enevoldsen I, Faber MH, Sørensen JD. Adaptative response surface techniques in reliability estimation. In: Schueller GI, Shinozuka M, Yao I, editors. Structural safety and reliability, 1994. p. 1257–64.

[11] Faravelli L. Response surface approach for reliability analysis. J Engng Mech 1989;115(12):2763–81.

[12] Hutchinson JW. Fundamentals of the phenomenological theory of nonlinear fracture mechanics. J Appl Mech 1983;50:1042–51.

[13] Kim SH, Na SW. Response surface method using vector projected sampling points. Struct Safety 1997;19(1):3–19.

[14] Krishnaswamy P, Scott P, Rahman S, et al. Fracture behavior of short circumferentially surface-cracked pipe. US Nuclear Regulatory Commission, Washington, DC, September 1995.

[15] Lemaire M. Finite element and reliability: combined methods by response surface. In: Frantziskonis GM, editor. Prabamat-21st Century: probabilities and materials, Dordrecht: Kluwer Academic, 1998. p. 317–31.

[16] Madsen HO. Omission sensitivity factors. Struct Safety 1988;5(1):35–45.

[17] Madsen HO, Krenk S, Lind NC. Methods of structural safety. Englewood Cliffs, NJ: Prentice-Hall, 1986.

[18] Mohamed A, Suau F, Lemaire M. A new tool for reliability based design with ANSYS FEA. ANSYS, Inc., ANSYS Conference and Exhibition, Houston, TX, USA, 1996. p. 3.13–3.23.

[19] Muzeau JP, Lemaire M, El-Tawil K. Méthode fiabiliste des surfaces de réponse quadratiques (srq) et évaluation des règlements. Construction Métallique (3), Septembre 1992.

[20] Olesen R. PROBAN User's Manual. Technical report, Det Norske Veritas Sesam, 1992.

[21] Pendola M. Couplage mécano-fiabiliste par surfaces de réponse. Application auxtuyauteries droites fissurées. Master's thesis, LaRAMA-Université Blaise-Pascal, Clermont-Ferrand, 1997.

[22] Rackwitz R, Fiessler B. Structural reliability under combined random load sequences. Computer Struct 1978:489–94.

[23] Rahman S, Brust FW, Ghadiali N, Choi YH, Krishnaswamy P, Moberg Brick-stad F, Wilkowski GM. Refinement and evaluation of crack-opening-area analyses for circumferential through-wall crack in pipes. US Nuclear Regulatory Commission, Washington, DC, April 1995.

[24] Rajashekhar MR, Ellingwood BR. new look at the response surface approach for reliability analysis. Struct Safety 1993;12(3):205–20.

[25] Rice JR. A path independent integral and the approximate analysis of strain concentrations by notches and cracks. J Appl Mech 1968:379–86.

[26] Rollot O, Pendola M, Lemaire M, Boutemy I. Reliability indexes calculation of industrial boilers under stochastic thermal process. Proceedings of the 1998 ASME Design Engineering Technical Conference, September 13–16 1998.

[27] Sih G. Mechanics of fracture. Vols. I–V. Leiden:Noordhoff, 1973–1977.